

A Method for Adaptive Time-Synchronized Measurement during Transients

K. Görner, M. Lechtenberg, Prof. Dr.-Ing. C. Rehtanz, Prof. Dr.-Ing. J. Götze

Abstract-- A precondition for precise measurement with PMUs (Phasor Measurement Units) is a quasi-stationary signal within the sampling data window. High accuracy is given as long as only electromechanical transients occur. However, electromechanical transients can be induced by switchings which cause electromagnetic transients as well. PMUs cannot always filter out these electromagnetic transients. Therefore, a new method for an adaptive time-synchronized measurement technique dealing with electromagnetic transients is discussed. The power system is modeled as a state-space model based on differential equations obtained by Kirchhoff's law in a linear RLC network. The solution of this state-space model contains voltages and currents as signal parameters. However, the stationary solution can only be obtained if the fundamental frequency is known in advance. Besides the fundamental frequency, a subspace-based frequency estimator like ESPRIT also provides other sub-synchronous resonance frequencies. These frequencies can be compared with the homogenous solution of the state-space model.

Keywords: Time-synchronized measurement, PMU, Transients, ESPRIT.

I. INTRODUCTION

Time-synchronized phasor measurement is regarded as beneficial for power system operation. It enables the monitoring of angle, frequency and voltage stability and has big potential for improvement of state estimation and power system restoration [1], [2]. In addition to monitoring, synchrophasors are considered as input for wide area control based on HVDC and FACTS [3] because of the high accuracy of the synchrophasors for quasi-stationary signals in accordance to the current IEEE standard C37.118.1 [3]. However, the evaluation of PMUs [5], [6] revealed that commercial PMUs may meet C37.118 requirements but are not capable of filtering out electromagnetic transients which occur during fast switchings or faults.

Therefore, this paper examines time-synchronized measurements disturbed by electromagnetic transients initiated by a switching. First of all, a signal model is needed so that

synchrophasors from the PMUs can be compared to a reference value. On the one hand, the IEEE standard defines the total vector error (TVE) for PMU accuracy. On the other hand, the standard does not describe how the reference value for TVE calculation is obtained. Numerical simulation enables off-line examination of electromagnetic transient signals. Usually, the solving is based on differential equations with the implicit trapezoidal rule of integration together with Bergeron's method for calculation of travelling waves [7]. Therefore, the numerical solution provides waveforms but does not provide output signal parameters such as damping, frequency, phase angle and amplitude which describe reference values for the evaluation of time-synchronized phasor measurement. A linear set of continuous time state-space formulations based on Kirchhoff's law in a linear RLC network must be solved in order to obtain these signal parameters.

The calculation of the synchrophasor very often applies the (discrete) Fourier transform (DFT) because of its efficiency for the determination of the fundamental component as long as the signal is stationary within its data window. However, a switching leads to non-stationary signals with non-harmonic frequency components. Subsequently, the additional signal components impede the fast measurement of the synchrophasor. In order to obtain meaningful synchrophasors, a detection of changes of the system state and a corresponding segmentation are required. To detect a change of state, an autocorrelation-based subspace analysis by the ESPRIT (Estimation of Signal Parameters Via Rotational Invariance Techniques) [8] algorithm can be applied, which can also be used to perform a continuous comparison to a-priori signal parameters. ESPRIT analyses the rotational invariance of temporarily subsequent eigenvectors to estimate the frequencies. With the help of the samples and the incorporated frequencies, the corresponding (initial) phase angles and amplitudes can be estimated. Furthermore, the time instant of system change can be estimated by monitoring confidence parameters like noise levels so that the non-stationary signal can be segmented and conventional algorithms such as DFT-based techniques can be applied [9].

Thus, adaptive time-synchronized measurement requires the consideration of the power system state. This can be done by a state-space formulation. Afterwards, specific algorithms can be applied. For the detection of electro-magnetic transients, ESPRIT is more suitable than the DFT since ESPRIT is based on a signal model which may consist of several non-harmonic frequencies. In contrast, the DFT is a mathematical transform and can only be used to estimate

This work was supported by the DFG (German Research Foundation). K. Görner and Prof. Dr.-Ing. C. Rehtanz are with ie³-Institute of Energy Systems, Energy Efficiency and Energy Economics, Dortmund, Germany (kay.goerner@tu-dortmund.de, christian.rehtanz@tu-dortmund.de) M. Lechtenberg and Prof. Dr.-Ing. J. Götze are with Information Processing Lab, TU Dortmund University, Dortmund, Germany (matthias.lechtenberg@tu-dortmund.de, juergen.goetze@tu-dortmund.de)

frequencies based on its sampling frequency and window length. It can be improved by interpolation methods [10], but it will still suffer from spectral masking.

This paper is organized as follows: Section II contains the description of the formulation of a continuous time state-space model and its solution. Section III is a review of the signal parameter estimation algorithm ESPRIT. The analysis of an event in an artificial 8-node network provides the non-perturbed signal parameters within Section IV. The closing of a transmission line is simulated in order to obtain typical signals of electromagnetic transients. The resulting signals are analyzed and evaluated by ESPRIT in Section V. These results are compared with the steady-state and with the results of DFT-based techniques. Moreover, Section V discusses the potential of signal segmentation. Section VI summarizes main results and highlights the advance of the estimation of subharmonics regarding time-synchronized phasor measurement during electromagnetic transients.

II. LINEAR STATE-SPACE SYSTEM MODEL

The linear state-space model will be exemplified by the switching of a transmission line to examine the influence of electromagnetic transients on the measurement of synchrophasors. The switching is chosen with respect to the constraint not to change the power balance significantly. By this, the generators and loads can be regarded as constant. Furthermore, the closing of a transmission line is symmetrical and (in contrast to breaking a line or a fault) the event cannot easily be detected by the zero component. We neglect the frequency dependency of the network's physical characteristics.

This suggests a one-phase linear state-space system model with constant parameters and excitation.

A. Model Description

The state of a power system is defined as a set of state variables enabling a complete mathematical description. This state-space model can be written as follows:

$$\dot{\vec{x}}(t) = A \vec{x}(t) + \vec{b}(t), \quad (1)$$

where $\vec{x}(t)$ is the state vector, A represents the system matrix and $\vec{b}(t)$ is the input vector representing external excitation.

A power system can be regarded as an interconnection of nodes. The nodes contain loads and generators and are connected by graphs. For these graphs, suitable transmission line models are chosen. Assuming a high meshed network like the European transmission network, the lines can be regarded electrically short. In consequence, we modeled the graphs with the PI-model. If a line is closed, the energizing of the line's capacitances should be taken into account. Since this cannot be modeled with PI, this line must be modeled as T-equivalent although its additional virtual node complicates the model. In exchange, the initial values of this line can be set to zero which is advantageous.

Two nodes ("i" and "j") and their connection are modeled by a RLC network as presented in Fig. 1.

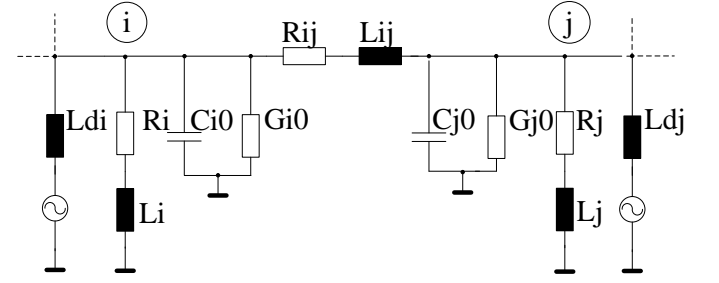


Fig. 1. Representation of power system by interconnected nodes (cut-out) with PI-modeled transmission line

The optional connection of a generator or load to a node is not necessary for the composition of the state-space model. A generator is modeled by a serial connection of a voltage source and an inductance. Loads are modeled by serial connection of resistance and inductance.

The state vector $\vec{x}(t)$ contains the currents in all generators $\vec{i}_G(t)$, loads $\vec{i}_L(t)$, transfer branches $\vec{i}_{ij}(t)$ and all nodal voltages $\vec{u}(t)$:

$$\vec{x}(t) = (\vec{i}_G(t); \vec{i}_L(t); \vec{i}_{ij}(t); \vec{u}(t)) \quad (2)$$

B. Solution of the State-Space Model

1) General Solution

Based on the homogenous differential equation system (3), eigenvalues and eigenvectors of the system can be obtained.

$$\dot{\vec{x}}(t) = A \vec{x}(t) \quad (3)$$

Every real eigenvalue λ_k of A with an associated eigenvector is a specific solution $w_k e^{\lambda_k t}$ of the differential equation set. For a complex eigenvalue $\lambda_k = a + jb$, a complex eigenvector $w_k = u + iv$ is determined. For its complex conjugate $\lambda_i = a - jb$, this can be done likewise. This results in two real solutions being the real part and the imaginary part of

$$\begin{aligned} w_k e^{\lambda_k t} &= (u + jv) e^{(a+jb)t} \\ &= e^{at} [u \cos bt - v \sin bt + j(v \cos bt + u \sin bt)]. \end{aligned} \quad (4)$$

There are n special real solutions where n is the dimension of the matrix A . The general homogeneous solution is a linear combination of the n special real solutions.

2) Particular Solution

The approach for the particular solution requires the consideration of $\vec{b}(t)$, the column vector of known functions of external excitation. These functions include the signals from the voltage sources in every node i :

$$u_{di}(t) = U_{di} \cdot \sin(\omega_i t + \varphi_i). \quad (5)$$

Each voltage source can be regarded as the excitation voltage of a generator. The vector $\vec{b}(t)$ may be composed of the sum of all terms containing excitation voltages multiplied with according topology parameters. Subsequently, the excitation vector can be composed by sine and cosine terms:

$$\vec{b}(t) = \sum_i (\vec{e}_i \cdot \sin(\omega_i \cdot t) + \vec{f}_i \cdot \cos(\omega_i \cdot t)). \quad (6)$$

Therefore, the approach for the particular solution is to define a solution for a state vector as follows:

$$\vec{x}_p(t) = \sum_i (\vec{c}_i \cdot \sin(\omega_i \cdot t) + \vec{d}_i \cdot \cos(\omega_i \cdot t)). \quad (7)$$

The vector elements in \vec{c}_i and \vec{d}_i are constants which can be calculated by the full solution and the initial state variable values. The particular solution can then be obtained by applying (7) in (1).

The resulting equation system can be separated in sine and cosine parts according to their frequency. It can be shown that for each frequency, the vector \vec{d}_i can be obtained by solving a linear system:

$$\underbrace{\left(-\frac{A^2}{\omega_i} \cdot -E \cdot \omega_i\right)}_{G_{Ai}} \vec{d}_i = \underbrace{\frac{A}{\omega_i} \cdot \vec{f}_i + \vec{e}_i}_{\vec{b}_{ef,i}}. \quad (8)$$

The vector \vec{c}_i can subsequently be obtained by:

$$\vec{c}_i = \frac{A}{\omega_i} \cdot \vec{d}_i + \frac{1}{\omega_i} \cdot \vec{f}_i. \quad (9)$$

3) Composition of full solution

As well known, the full solution of the differential equation system can be obtained by the summation of the general and particular solution. The general solution represents additional signal components – electromagnetic transients, which are very often regarded as noise. These signals can be assumed to be damped. The particular solution represents the stationary solution, which contains synchrophasor information. In consequence, with the first sample which detects the switching, we can theoretically calculate the resulting stationary value. Subsequently, stationary parameters such as angle and magnitude for each signal can be obtained.

This implies that the stationary value can be regarded as constant right before and after the event.

C. Example: Simulation of Switching

To prove the concept, the closing of a parallel transmission line in a two-node system as displayed in Fig. 2 is simulated exemplarily. In this scenario, two generators are connected via one transmission line. A load is connected to node 2. The resulting power flow leads to a quite low voltage in node 2. Therefore a parallel transmission is closed at time $t=2.005$ s.

Keeping in mind that we focus on the fundamental phasor, we validated the stationary values by stationary complex calculation.

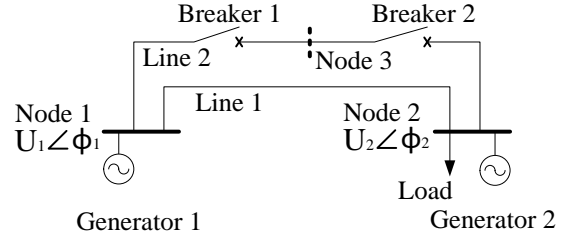


Fig. 2. Scenario to prove the legitimacy of the calculation of electromagnetic transients by the analytical solution of state-space formulation

To take the energizing of the capacitance in line 2 into account, a T-equivalent network must be applied. Only with this, the initial values for an unloaded capacitance can be applied, i.e. the voltage of the capacitance is zero. Topology parameters are given in the Appendix.

Fig. 3 displays the resulting voltage step of the fundamental 50-Hz-component. The closing at time $t=2.005$ s of a line leads to an increase of the nodal voltage magnitudes.

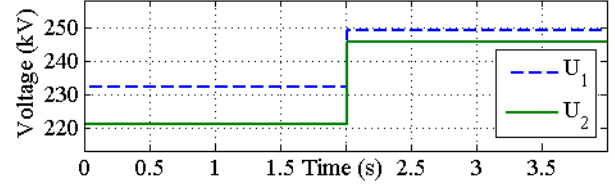


Fig. 3. Fundamental voltage magnitude during closing of parallel transmission line in two-node system

Simultaneously, the phase angle of both nodal voltages drops as displayed in Fig. 4.

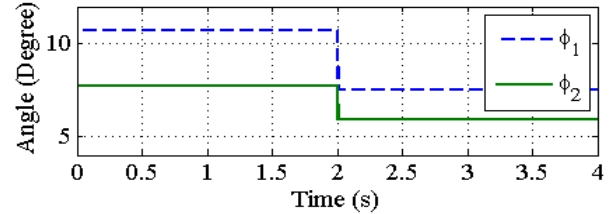


Fig. 4. Fundamental voltage angle during closing of a parallel transmission line in two-node system

However, the complete resulting signal includes the electromagnetic transients as well, see Fig. 5. Right after the closing at $t=2.005$ s, both instantaneous voltages drop because of the energizing of the line capacitance.

In node 2, the voltage is damped because of the impedance of the connected load.

At node 1, no additional components damp the high frequency oscillation so that these signal components disturb the fundamental 50 Hz significantly for more than one cycle.

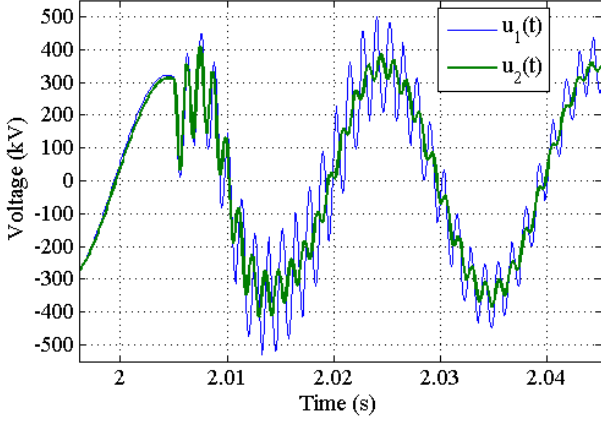


Fig. 5. Voltage waveform during the switching and energizing the parallel transmission line

Though this example only utilizes a small model, we can conclude that topology changes can lead to heavy disturbances caused by electromagnetic transients. In consequence, small changes of magnitude or phase angle cannot easily be detected. However, from the state-space calculation we know that the stationary value exists immediately after the switching. Furthermore, the stationary value can be estimated by the particular solution of state-space model depending on topology information and excitation values as well as the system frequency.

III. PARAMETER ESTIMATION

For the examination of the influence of electromagnetic transients on synchrophasor measurements, the mentioned state-space model (1) can be connected with a parameter estimation algorithm. As mentioned, there are two intersections. Prior to the state-space estimation, the fundamental system frequency can be estimated and then be used as initial value for the state-space estimation. After the state-space estimation, the remaining parameters of the signal can be estimated and matched to the results of the state-space estimation to verify the results in-the-loop. A suitable parameter estimator is the subspace-based parameter estimation using the eigenvectors of the samples' autocorrelation matrix to estimate the incorporated sinusoids, i.e. ESPRIT [11]. In this work, we propose to use an extended approach named DaPT [12] which is able to handle a variable number of sinusoids with various intensities. The general signal model for the input samples y used for ESPRIT can be written as follows:

$$\begin{aligned}
 y &= w_{\text{awgn}} + \sum_{i=1}^p a_i e^{j(2\pi m \frac{f_i}{f_s} + \phi_i)} \\
 &= w_{\text{awgn}} + \sum_{i=1}^p c_i e^{j2\pi m \frac{f_i}{f_s}} \quad ; \quad c_i = a_i e^{j\phi_i}.
 \end{aligned} \quad (10)$$

Within this equation, w_{awgn} denotes additional white Gaussian noise, p represents the rank with the according parameters for frequency, phase and amplitude (f_i , ϕ_i , a_i).

The sampling frequency is noted as f_s and the time-index is m . Reconsidering Eq. (4), the solutions of the state-space model describe sine functions (so-called sinusoids). In a potential voltage measurement, these sinusoids appear superposed. To map this to the signal model of Eq. (10), it is considered that every sinusoid can be written as the sum of two complex exponential functions (Euler's identity). In addition, the DC offset of such measurement has the frequency $f_{\text{DC}} = 0\text{Hz}$ making it a constant. This results in the following model specific to this application:

$$y = w_{\text{awgn}} + C_{\text{DC}} + \sum_{i=1}^r \hat{C}_i \left(e^{j2\pi m \frac{f_i}{f_s}} + e^{j2\pi m \frac{-f_i}{f_s}} \right). \quad (11)$$

In this equation, the new parameter $r = 0.5(p - 1) + 1$ numbers the superposed sinusoids. The frequencies of the superposed sinusoids incorporated in a voltage measurement of a node are estimated via a subspace-based approach. A sliding vector of temporally equidistant and subsequent samples \vec{y} is used to estimate the autocorrelation matrix of the measurement signal. Typically, this is done via exponential averaging: $R_{yy,m} = \beta R_{yy,m-1} + \vec{y} \vec{y}^H$.

An eigenvector analysis of the autocorrelation matrix reveals the sinusoids of which the signal is composed. The common ESPRIT algorithm enables the parameter extraction from such eigenvector by estimating the rotation (in the sense of complex exponentials) needed to shift the phase as much as one time-step ($t_s = f_s^{-1}$) does. This principle is called rotational invariance. The challenge is the varying rank r of the signal; every event-driven sinusoid beside the fundamental component is only temporarily present. This rank is not available a-priori and has to be estimated. However, the statistical distribution of the sinusoids' amplitudes is not suitable for common rank estimators like AIC/MDL [13]. To overcome this, the rank is always overestimated a little so that ESPRIT will calculate *noise frequencies*. Rating ESPRIT's results over time can identify and separate signal frequencies from noise and – by counting these – provide a rank estimation. The procedure is realized in DaPT. In addition, this tool chain may be extended with functions to enforce the estimation and extraction of DC-offsets and to specially look for a-priori known, possible frequencies like the fundamental frequency and the frequencies incorporated in the solution of the state-space model (recursive approach) [14].

The signal model from Eq. (11) can be used to estimate each frequency's phasor (c_i). After the frequency estimation, all elements of the equation are known except of the complex amplitudes and the noise. Since the input samples are provided as a window of data and the time index for each sample is known, the signal model becomes an over-determined set of equations that can be solved with respect to the minimal squared error by e.g. Least-Squares.

This approach provides viable results using the fundamental component as only input. However, the error can be reduced if the results of ESPRIT are incorporated. Moreover, information on the strength of subharmonic frequency components can be extracted.

This solution can obviously only be valid if the signal can be assumed quasi-stationary for the data window. Fortunately, this solution can also be used to reconstruct the signal. This enables the calculation of the mentioned squared error, which can easily be used to perform segmentation.

IV. SIMULATION

To examine different damped signals, the closing of a parallel transmission line in an eight-node system is simulated. The model is displayed in Fig. 6. The size of this system might seem small, but it is complex enough to demonstrate our method. In an interconnected network, signals are disturbed differently depending on topology and the distance from the place of origin. It is shown that the change of the system state can be detected by signal processing algorithms within fractions of a cycle.

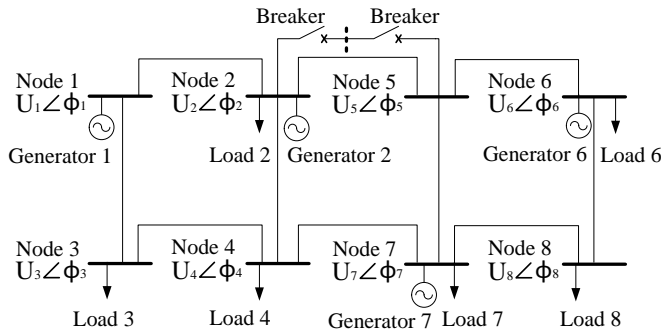


Fig. 6. Eight-node system for simulation of electromagnetic transients

In the following scenario, the voltage in node eight on the bottom right of the system is below 0.9 p.u. (ca. 207 kV), see Fig. 7. The closing of a parallel transmission line at time $t=2.005$ s leads to an increase of all voltages across the network. Especially at node 8, the voltage rises above 0.9 p.u. into operational limits.

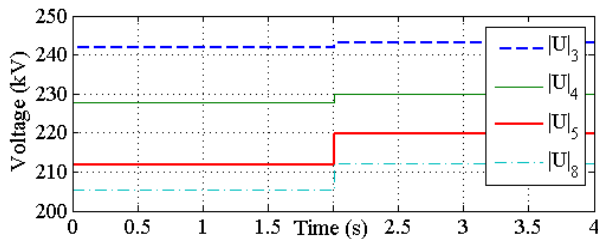


Fig. 7. Stationary value of nodal Voltage before and after switching

The switching causes sudden changes of the phase angle as well, see Fig. 8. However, the change might be very small. E.g. the voltage phase angle in node five only drops around 0.07 degrees. On the other hand, the phase angle in node 3 rises around 0.3 degrees.

As long as the fundamental values are obtained from the simulation, small variations in angle and magnitude can be recognized.

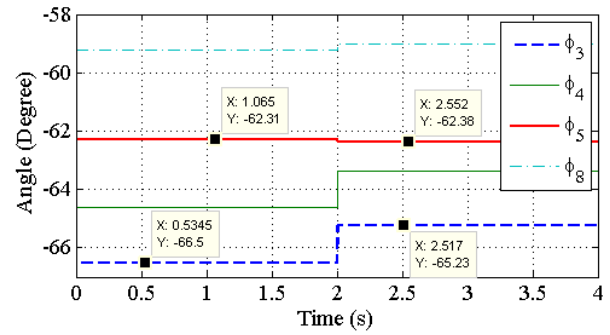


Fig. 8. Angle of fundamental component before and after switching

The transient voltage waveform reveals that in a short period electromagnetic transients disturb the fundamental value. The voltage at more distant places, i.e. nodes with a larger (multi-hop) distance to the origin of the disturbing event, is less disturbed as shown in Fig. 9.

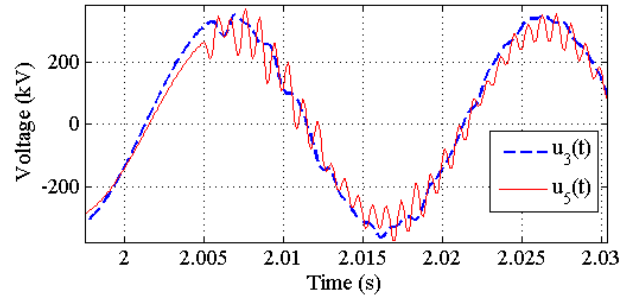


Fig. 9. Transient voltage waveform during switching

A cut-out of the voltage waveforms of different nodes shows that the additional disturbing signals occur later for distant nodes. For example in Fig. 10, the distortion of the voltage occurs first at node 5 which is close to the switched line; then the distortion occurs in nodes four, eight and three subsequently.

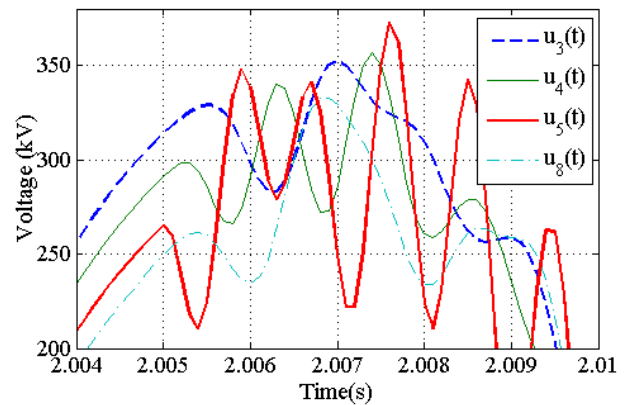


Fig. 10. Zoom in Transient voltage waveform during switching

V. SIGNAL ANALYSIS

The frequency analysis of the voltage signal $u_5(t)$ using ESPRIT is shown in Fig. 11. Two strong frequency components are detected shortly after energizing the parallel line at $t=2.005$ s.

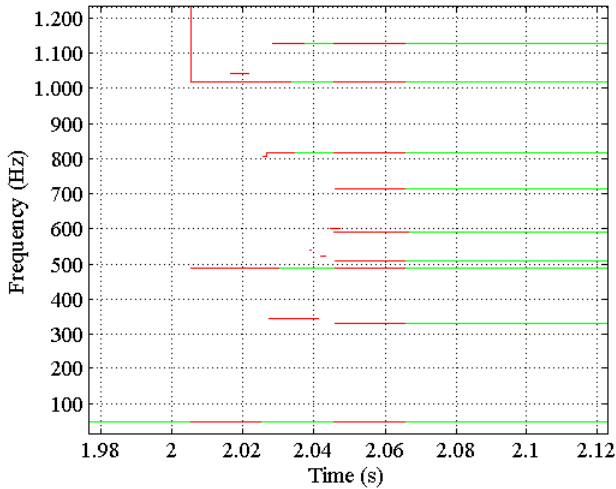


Fig. 11. Frequency analysis with ESPRIT for $u_5(t)$

However the estimated frequencies are marked (red) with a higher grade of uncertainty for around 20 ms. With 20 ms delay, other subharmonic frequency components are detected, too. Such a high number of different additional frequencies are a clear sign indicating a non-stationary signal. In consequence, the signal should be segmented at $t=2.005$ s with the occurrence of the first higher harmonics. The MSE-level of the Least-Squares-based phasor estimation will trigger the event at about the same time. Choosing a small window length for the Least-Squares estimator, the segmentation can be triggered even earlier. An adaptive segmentation approach will be a topic of further research.

The plot of the calculated phase angle in Fig. 12 shows that a segmented signal is a precondition for high accuracy in contrast to ordinary sliding windows. Furthermore, the comparison of rectangular and hamming windows reveals that even the window type does not matter. This is consistent due to the constraint of stationary signals. Only the angle calculation of the (segmented) Least Squares phasor estimation shows a fast response but undershoots for 40 ms.

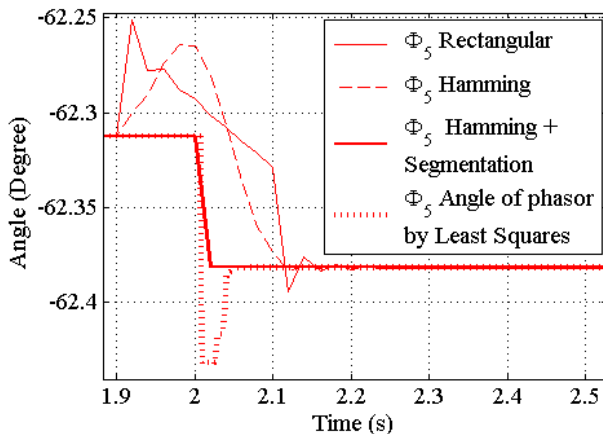


Fig. 12. Comparison of angle measurements of $u_5(t)$ during switching analyzed by DFT with different windows and optional segmentation

As mentioned before, the distortion is much less in remote sites like node three (see Fig. 13). Frequency components with

higher frequency are detected with a delay of around 30 ms even though we know from Fig. 10 that the waveform is distorted right after the switching at $t=2.005$ s. The reasons for this are the small amplitudes of the additional components at such distant site which renders the frequency estimation uncertain during this delay.

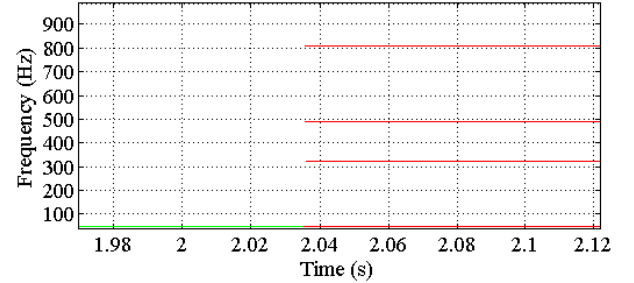


Fig. 13. Frequency analysis with ESPRIT for $u_3(t)$

The angle's step is still detected but with a delay (Fig. 14). If the segmentation error can be corrected for example by refreshed information from other nodes then the angle can be detected precisely as well using DFT.

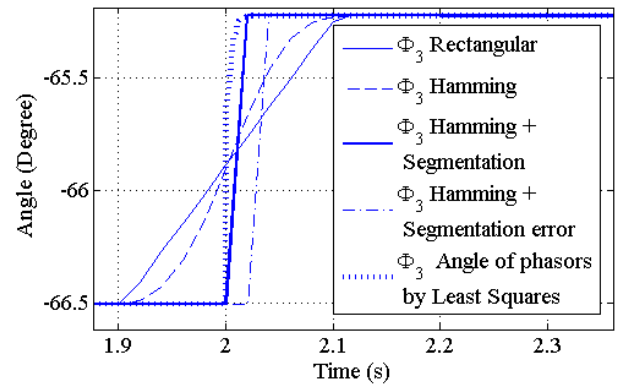


Fig. 14. Comparison of angle measurement of $u_3(t)$ during witching analyzed by DFT with different windows and optional segmentation

As an alternative, the least squares method provides fast and accurate angle estimation without overshoot. As can be seen in Fig. 15, the mean square error between the measurement and a reconstructed signal based on the least squares estimation easily provides segmentation information.

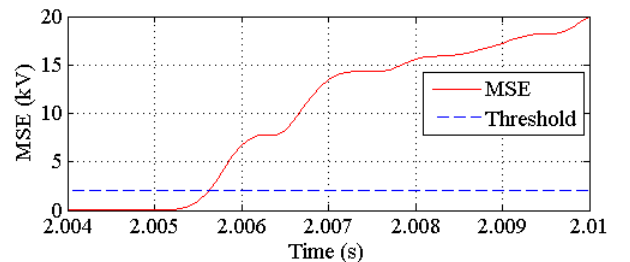


Fig. 15. Mean square error of reconstructed signal against measurement

VI. RESULTS

Based on the signal analysis in the previous chapter, we conclude that time-synchronized phasor measurement is not disturbed by electromagnetic transients as long the non-stationary signal is segmented into quasi-stationary segments.

In consequence, each data window of one segment does not contain different system states. If the segmentation is done correctly at the right time instant, conventional signal processing algorithms like DFT-based techniques can provide high accuracy.

ESPRIT is an efficient algorithm for the detection and identification of additional signal components. This information can be valuable for the assessment of the power system (e.g. event classification). In case of strong disturbances, the frequency estimates can help isolating the fundamental component by supporting a Least Squares-based phasor estimation.

Both algorithms provide powerful information for the segmentation. Furthermore, the validity of the synchrophasor can be flagged or marked in a way that as long as subharmonic frequency components are detected the input signal is not a stationary single-sinusoid signal. Moreover, ESPRIT is a more suitable tool for the analysis of electro-magnetic transients than the (discrete) Fourier transform because it has higher resolution and is not sensible to spectral masking, i.e. signals with frequencies which are close together can be detected, too.

VII. REFERENCES

- [1] Novosel, D.; Madani, V.; Bhargava, B.; Khoi Vu; Cole, J.; , "Dawn of the grid synchronization," *Power and Energy Magazine, IEEE* , vol.6, no.1, pp.49-60, January-February 2008 doi: 10.1109/MPAE.2008.4412940
- [2] Bose, A.; , "New computer applications for system operations using phasor measurements," *Power and Energy Society General Meeting, 2012 IEEE* , vol., no., pp.1-5, 22-26 July 2012
- [3] Yong Li; Rehtanz, C.; Ruberg, S.; Longfu Luo; Yijia Cao; , "Wide-Area Robust Coordination Approach of HVDC and FACTS Controllers for Damping Multiple Interarea Oscillations," *Power Delivery, IEEE Transactions on* , vol.27, no.3, pp.1096-1105, July 2012
- [4] "IEEE Standard for Synchrophasor Measurements for Power Systems," *IEEE Std C37.118.1-2011 (Revision of IEEE Std C37.118-2005)* , vol., no., pp.1-61, Dec. 28 2011
- [5] Balabin, M.; Görner, K.; Li, Y.; Naumkin, I.; Rehtanz, C.; , "Evaluation of PMU performance during transients," *Power System Technology (POWERCON), 2010 International Conference on* , vol., no., pp.1-8, 24-28 Oct. 2010
- [6] Kamwa, L.; Samantaray, S. R.; Joos, G.; , "Compliance Analysis of PMU Algorithms and Devices for Wide-Area Stabilizing Control of Large Power Systems," *Power Systems, IEEE Transactions on* , vol.PP, no.99, pp.1-13, 2012
- [7] Dommel, H.W.; , "Techniques for analyzing electromagnetic transients," *Computer Applications in Power, IEEE* , vol.10, no.3, pp.18-21, Jul 1997
- [8] R. Roy, T. Kailath : "ESPRIT- Estimation of Signal Parameters via Rotational Invariance Techniques ". *IEEE Trans. on Acoustics, Speech, and Signal Processing*, Vo1.37,N. 7, July 1989, pp 984-995
- [9] A.G. Phadke, J.S. Thorp, "Synchronized Phasor Measurements and Their Applications", Springer Science+Business Media, LLC 2008
- [10] Quinn, B.G.; , "Estimation of frequency, amplitude, and phase from the DFT of a time series," *Signal Processing, IEEE Transactions on* , vol.45, no.3, pp.814-817, Mar 1997
- [11] Akaike, H. *Information Theory and an Extension of the Maximum Likelihood Principle*. International Symposium on Information Theory, (S. 267-281). Tsahkadsor, Armenian SSR, 1973
- [12] Lechtenberg, M., & Götze, J. Database Assisted Frequency Estimation. 4th IEEE International Conference on Computer Science and Information Technology. Chengdu, Sichuan, China, June 2011

- [13] Lechtenberg, M., Götze, J., Rehtanz, C., & Görner, K.. Estimation of Oscillation Parameters for Power Grids. 2012 IEEE Asia Pacific Conference on Circuits and Systems. Kaohsiung, Taiwan, December 2012
- [14] Paulraj, A., Roy, R., & Kailath, T.. A subspace rotation approach to signal parameter estimation. *Proceedings of the IEEE*, 74(7), 1044-1046, July 1986

VIII. APPENDIX

Topology data for calculation in Section II.C:

TABLE I: GENERATOR DATA

Node number	Ld [H]	Udi [kV]	ϕ [°]	f [Hz]
1	0.92	350	30	50
2	0.92	350	30	50

TABLE II: LOAD DATA

Node number	R [Ω]	L [H]
2	325.80	0.340866

TABLE III: LINE DATA

Node i	Node j	R[Ω]	L[mH]	C[μ F]	G[S]
1	2	6.65	139.26	2.40	0
1	3	3.325	69.63	1.20	0
3	2	3.325	69.63	1.20	0